Multiple Characterization for Mechanistic Insights of Pb(II) Sorption onto Biochars Derived from Herbaceous Plant, Biosolid, and Livestock Waste

Zhuhong Ding,[a,*] Hailu Wu,[a] and Xin Hu [b]

Biochars are considered as promising sorbents for the removal of aqueous metal ions. The aim of this study was to explore the adsorption mechanisms through the integrated characterization of the pristine and Pb(II)-loaded biochars derived from herbaceous plant, biosolid, and livestock waste with different physicochemical properties. The biochar derived from livestock waste exhibited higher Pb sorption capacity than the others. Experimental data of sorption kinetics and isotherms were well fitted by kinetic models and Langmuir isotherm model, respectively. Comparisons of Fourier-transform infrared spectroscopy (FT-IR), X-ray powder diffraction (XRD), and X-ray photoelectron spectroscopy (XPS) between the pre- and post-adsorption biochars revealed the formation of Pb-carbonate, suggesting that the surface precipitation was the dominant adsorption mechanism. The combination of multiple characterizations and batch adsorption can make further exploration on the adsorption mechanism of Pb(II) adsorption onto the resultant biochars.

Keywords: Physicochemical property; Batch sorption; X-ray photoelectron spectroscopy; Sorption mechanism

*Contact information: a: School of Environmental Science & Engineering, Nanjing Tech University, 30 Puzhu Southern Road, Nanjing 211816, P.R. China; b: State Key Laboratory of Analytical Chemistry for Life Science, Center of Material Analysis, 20 Hankou Road, Nanjing University, Nanjing 210093, P.R. China; *Corresponding author: dzhuhong@njtech.edu.cn*

INTRODUCTION

Biochars, synthesized through slow pyrolysis or carbonization of feedstock biomass in an oxygen-limited environment, have received increasing attention for their potential environmental benefits such as carbon sequestration, soil fertility improvement, and pollution remediation (Ahmad *et al.* 2014; Mohan *et al.* 2014; Inyang *et al.* 2016). In particular, biochars have been used as low-cost, sustainable adsorbents to remove organic and inorganic contaminants from aqueous solutions (Mohan *et al.* 2014; Inyang *et al.* 2016). Current literature has covered a wide spectrum of biochars derived from various biomass feedstocks such as pine wood, oak wood, hard wood, corn straw, soybean straw, orange peel, anaerobically digested sugarcane bagasse, cow manure, sugar beet tailing, and coconut coir (Tan *et al.* 2015; Inyang *et al.* 2016). They can be simply classified as plant-based, sludge-based, and manure-based biochars. Traditionally, the basic physicochemical properties of these resultant biochars were analyzed or characterized firstly, which includes contents of C, H, N, and mineral elements, specific surface areas, surface functional groups, crystalline phases, and thermal stability, and morphology; and then batch sorption experiments (adsorption isotherm, kinetics and/or thermodynamics) and/or column sorption experiments were carried out to investigate the adsorption performance and the

empirical or semi-empirical mathematical models such as the Langmuir isotherm equation, Freundlich isotherm equation, pseudo-first-order equation, and pseudo-second-order equation were used to fit the experimental data to discuss the adsorption mechanisms (Mohan *et al.* 2014; Inyang *et al.* 2016). For example, kinetic experiments of metal ions sorbed onto various biochars have shown that the pseudo-second-order model fits the data better than the first-order model (Mohan *et al.* 2014; Inyang *et al.* 2016). The equilibrium sorption isotherms are fitted with Langmuir, Freundlich, and Dubinin-Radushkevich (D-R) isotherm models, reflecting the sorbent surface properties and the affinity of contaminants to the biochars (Mohan *et al.* 2014; Inyang *et al.* 2016).

The common instrumental characterizations used in the various biochars include scanning electron microscope equipped with an energy-dispersive spectrometer (SEM-EDS), thermogravimetric analyzer (TGA), Fourier transform infrared spectra (FTIR), X-ray diffraction (XRD), CHN elemental analyzer, inductively coupled plasma optical emission spectroscopy (ICP-OES), and X-ray photoelectron spectroscopy (XPS) (Chen *et al.* 2015; Ding *et al.* 2016b; Fu *et al.* 2016; Xu *et al.* 2017). These characterizations can reveal the physicochemical properties of biochars, which have great influences on the adsorption capacities of metal ions onto biochars (Ahmad *et al.* 2014; Mohan *et al.* 2014; Inyang *et al.* 2016). Now they were used further to explore the adsorption mechanisms through the comparison of the pristine and the adsorbate-loaded biochars (Hu *et al.* 2015; Xu *et al.* 2017). Therefore, the combination of batch sorption and integrated characterization techniques may be more effective in identifying the governing adsorption mechanisms of contaminants onto the biochars and further study should be carried out on the biochars derived from different biomass feedstock.

In the present study, plant-based, sludge-based and manure-based biochars were derived from herbaceous plant (Spanish moss), biosolid, and livestock waste, respectively. Pb(II), one of the most investigated metal ions adsorbed by biochars (Ding *et al.* 2016a; Inyang *et al.* 2016; Chen *et al.* 2017), was selected as a represented heavy metal ion. Batch isotherm and kinetic sorption experiments were performed. The pristine and the Pb(II)-loaded biochar samples were analyzed using bulk and surface characterization techniques such as FT-IR, XRD, and XPS. The object of this study was to explore the adsorption mechanisms through the combination of batch sorption and integrated characterization.

EXPERIMENTAL

Chemical reagents

Analytical reagents including NaOH, HNO_3, $Pb(NO_3)_2$ were purchased from Sinopharm Chemical Reagent Co., Ltd. (Shanghai, China). Solutions were prepared using ultrapure water (18.2 MΩ*cm) (Milli-Q Advantage A10 System, Darmstadt, Germany).

Preparation of Sorbents

The herbaceous plant (Spanish moss) was collected from the campus of the University of Florida (UF) in Gainesville, FL, USA. The biosolid (sludge) was collected locally in Gainesville, FL, USA. The livestock waste was obtained from a local livestock breeding plant in Gainesville, FL, USA. Each biomass was ground in a knife mill (Model No. 4, Arthur H. Thomas Company, Philadelphia, PA, USA) into powder. The powders were placed inside tubular quartz reactors and then inserted into a benchtop muffle furnace (Barnstead 1500 M, Auburn, AL, USA) purged with N_2 gas.

The pyrolysis furnace temperature was increased at a rate of 20 °C/min and then held at 600 °C for 2 h with flowing N_2 gas. The obtained samples were rinsed with tap water and DI water and then oven dried at 80 °C. The pristine biochars were placed in zipper bags and denoted as SM (Spanish moss), BIOS (biosolid), and MAW (mixed animal waste). The details are given in a previous report (Wu *et al.* 2016)

Batch Aqueous Pb(II) Sorption

Batch sorption experiments consisted of an isotherm test and a kinetic test. All experiments were carried out at room temperature (22 ± 2 °C) by adding 0.05 g sorbent to 100 mL polyethylene centrifuge tubes containing 50 mL Pb(II) solution prepared from $Pb(NO_3)_2$ with pre-defined concentrations. The solution pH was adjusted to 5.5 ± 0.2 using 0.01 mol L^{-1} NaOH and 0.01 mol L^{-1} HNO_3. After shaking for a pre-defined contact time in a rotary shaker, the mixture was centrifuged at 4000 rpm for 10 min. The concentrations of Pb(II) in the supernatants were determined using inductively coupled plasma optical spectrometry (ICP-OES, Optima 5300, Perkin-Elmer, Waltham, MA, USA). The amount of adsorbed Pb(II) (q_t or q_e) per unit adsorbent mass were calculated using the following equation,

$$q_t = [(C_0 - C_t)\, V]/m \quad (1)$$

where C_0 and C_t are the concentrations of Pb(II) at time 0 and t (mg L^{-1}), respectively; q_t is the amount adsorbed (mg g^{-1}) at contact time t (q_e is q_t at equilibrium time); V is the volume of the solution (L); and m is the mass of the adsorbent (g).

The initial concentrations for the isotherm test were set at 0.5 mg·L^{-1}, 5 mg·L^{-1}, 10 mg·L^{-1}, 25 mg·L^{-1}, 50 mg·L^{-1}, and 100 mg·L^{-1} with shaking times of 24 h. In the kinetic sorption test, the contact time was set as 5 min, 15 min, 30 min, 45 min, 60 min, 120 min, 240 min, 360 min, 480 min, 720 min, and 1440 min at pH of 5.5 ± 0.2 with Pb(II) concentrations of 10 mg·L^{-1} and 50 mg·L^{-1}. All the adsorption experiments were conducted in duplicate and the mean values were reported. The sorption experiments without spiked Pb ([Pb(II) = 0 mg·L^{-1}]) were used as control groups.

Characterization of the Pre- and Post-Sorption Biochars

The basic physicochemical properties of the resultant biochars (*e.g.*, contents of C, H, N, and mineral elements, pH value of the point zero charge (pH_{PZC}), specific surface areas, thermogravimetry analysis, and morphology) were presented in an earlier report (Wu *et al.* 2016).

The infrared spectra of the pristine and the post-sorption biochars were recorded using a Fourier-transform infrared spectroscopy (FT-IR, NEXUS870, NICOLET Co., Madison, WI, USA) in the range of 4000 cm^{-1} to 500 cm^{-1} with a resolution of 0.2 cm^{-1}, using a KBr disc containing 1% of finely ground sample produced *via* bench press. Crystalline minerals in the pristine biochar and the post-sorption biochars were detected using X-ray Powder Diffraction (XRD) (XRD-6000, Hitachi Co., Tokyo, Japan).

The composition of surface elements and Pb speciation in biochar samples were analyzed using X-ray photoelectron spectroscopy (PHI 5000 VersaProbe, UlVAC-PHI, Maoqi, Japan).

RESULTS AND DISCUSSION

Batch Sorption Kinetics and Isotherm

The sorption of Pb(II) onto the biochars increased considerably with increasing contact time in the course of the first hour and then slowed until reaching an equilibrium (Fig. 1a). Low initial concentrations of Pb(II) reached equilibrium adsorption more readily than high initial concentrations (Fig. 1a). However, the sorption curve of 10 mg L^{-1} Pb(II) shifted unexpectedly, which might be due to the higher adsorption capacity of MAW for Pb(II). Also, most of the Pb(II) at lower initial concentrations was adsorbed at earlier contact time. The pseudo-first-order and pseudo-second-order model both were well fitted to the experimental data to characterize the sorption kinetics of Pb(II) ions onto biochars (Table 1). The pseudo-second-order kinetic model provided a somewhat better fit, except for that for 10 mg L^{-1} Pb(II), which is in agreement with previous research on sorption characteristics ((Tan *et al*. 2015).

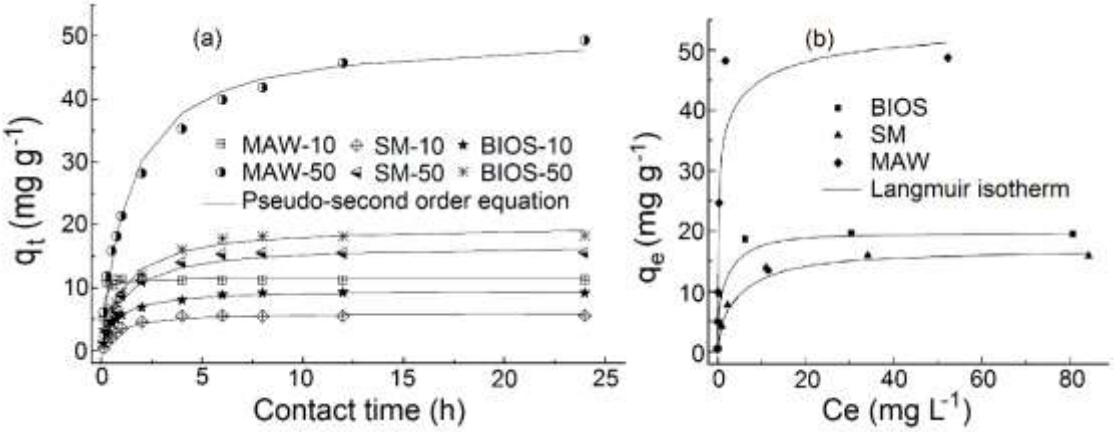

Fig. 1. Sorption kinetics (a) and isotherm (b) of Pb(II) onto the resultant biochars

Table 1. Kinetic Parameters for Pseudo-First-order and Second-order Kinetic Models for the Adsorption of Pb(II) onto the Biochars

	Initial con.	$q_{e\text{-}exp}$	Pseudo-first-order			Pseudo-second-order		
	(mg/L)		$1/q_t = 1/q_e + k_1/(q_e t)$			$t/q_t = 1/[(q_e)^2 \times k_2] + t/q_e$		
			$q_{e\text{-}cal}$	K_1	R^2	$q_{e\text{-}cal}$	$K_2/10^{-4}$	R^2
MAW	10	11.2	11.2	7.95	0.913	11.6	12.9	0.776
	50	49.2	44.8	0.60	0.934	50.4	0.15	0.981
SM	10	5.55	5.54	0.97	0.997	6.09	2.06	0.983
	50	15.6	15.0	0.75	0.984	16.9	0.54	0.994
BIOS	10	9.17	8.81	1.11	0.967	9.64	1.48	0.995
	50	18.3	17.9	0.73	0.975	20.1	0.47	0.986

K_1 and K_2: the rate constant of the pseudo-first-order equation (min^{-1}) and the pseudo-second-order equation (g mg^{-1} min^{-1}), respectively.

The equilibrium sorption capacities differed among different biochars (Fig. 1b). MAW shows the maximum sorption capacities while SM exhibits the least (Fig. 1b). The equilibrium sorption isotherms reflect the sorbent surface properties and Pb (II) affinity for the biochars. Langmuir, Freundlich, and Dubinin-Radushkevich (D-R) isotherm models were used to fit the isotherm data accordingly. The coefficients of determination (R^2) listed

in Table 2 indicated good fitting with these isotherm models ($R^2 > 0.80$), with the Langmuir adsorption isotherm being a generally better model. The Langmuir adsorption capacities for Pb (II) were 16.8 mg g^{-1} for SM, 19.6 mg g^{-1} for BIOS, and 51.5 mg g^{-1} for MAW (Table 2). The observed values were larger than most of the reported values in the literature such as 4.13/3.00 mg g^{-1} for pine wood/bark char, 2.62/13.10 mg g^{-1} for oak wood/bark char (Mohan *et al*. 2007), 3.89 mg g^{-1} to 4.25 mg g^{-1} for pine wood biochar, and 1.84 mg g^{-1} to 2.40 mg g^{-1} for rice husk biochar (Liu and Zhang 2009). Based on the Langmuir constant (K_L) and the initial Pb(II) concentration (Co), the dimensionless separation factor (R_L) can be calculated ($R_L = 1 / (1 + K_L C_0)$). It is believed that R_L value indicates the type of isotherm to be irreversible ($R_L = 0$), favorable ($0 < R_L < 1$), linear ($R_L = 1$), or unfavorable ($R_L > 1$). The R_L values for the adsorption of Pb(II) onto the biochars for all studied initial Pb(II) concentrations were below 1, indicating that the sorption of Pb(II) was a favorable process. Single point adsorption distribution coefficients (K_d) at low and high equilibrium concentrations (C_e = 5 and 50 mg L^{-1}) are used to judge sorption ability. K_d values in Table 2 show that the sorption ability was in the order of MAW > BIOS > SM.

The slope of $1/n$ of the Freundlich model indicates a normal Freundlich isotherm when $1/n < 1$ and cooperative adsorption when $1/n > 1$. The range between 0.1 and 0.8 for $1/n$ in the present study (Table 2) is indicative of easy adsorption of Pb (II) onto biochars. The sorption mean free energy (E) from the D-R isotherm model ($E=1/\sqrt{2\beta}$) can be used to evaluate whether physical sorption ($E < 8$ kJ/mol) or chemical sorption (8 kJ/mol $< E <$ 16 kJ/mol) is the predominant sorption mechanism (Helfferich 1962). The E values were 12.1 KJ/mol, 8.34 KJ/mol, and 8.27 KJ/mol for the sorption of Pb(II) onto MAW, SM, and BIOS, respectively (Table 2), suggesting the chemical mechanisms.

Table 2. Isotherm Model Parameters for Pb Sorption onto Biochars

	Langmuir Isotherm			K_d (L/g)		Freundlich Isotherm			D-R Isotherm		
	$C_e/q_e = C_e/q_m + 1/(K_L \times q_m)$			$K_d = Q_e/C_e$		$\lg q_e = \lg K_F + (1/n)\lg C_e$			$\lg q_e = \ln q_m + \beta[RT\ln(1+1/C_e)]^2$		
	q_m	K_L	R^2	C_e=5	C_e=50	K_F	1/n	R^2	q_m	β	R^2
MAW	51.5	3.34	0.984	9.72	1.02	5.63	0.76	0.928	56.8	3.42×10^{-9}	0.889
SM	16.8	0.38	0.997	2.20	0.32	6.28	0.24	0.900	18.2	7.20×10^{-9}	0.976
BIOS	19.6	2.83	0.983	3.70	0.39	10.2	0.18	0.863	18.9	7.31×10^{-9}	0.972

q_m: Maximum adsorption capacity (mg g^{-1}); K_L: Langmuir constant (L mg^{-1}); R^2: coefficient of determination; K_F: affinity coefficient related to the bonding energy ($mg^{(1-1/n)}$ $L^{1/n}$ g^{-1}); n: the heterogeneity factor that represents the bond distribution; β: the isotherm constant $(mol/J)^2$; R: the gas constant (8.314 J/mol K); and T: absolute temperature (K).

FT-IR Spectra of the Biochars

FT-IR spectra (Fig. 2a) were used to obtain information about the kinds of the functional groups and their chemical environment located for the pre- and post-sorption biochars. In Fig. 2a, the broad band at 3200 cm^{-1} to 3500 cm^{-1} was assigned to OH groups. The broad bands at ~1710 cm^{-1} and ~1600 cm^{-1} represented carboxyl groups. The broad bands at ~1430 cm^{-1} were assigned to asymmetric C–O stretching in carbonates. Finally, the peaks at 890 cm^{-1}, 820 cm^{-1}, and 760 cm^{-1} were assigned to the aromatic C−H bonding for all the tested biochars. The FT-IR spectra of the pre- and post-sorption biochars were very similar. The lack of obvious shift on the FT-IR spectra after adsorption may have been due to the strong light absorption of black biochars, which may have concealed the slight shift effect caused by the limited metal adsorption amount. For example, Table 2 showed that the adsorption amounts for Pb (II) were all below 6%. Also, it is known that FTIR

gives information mainly about bulk properties, and changes associated with interactions at the surface of black biochars can be hard to detect. Similar results were reported previously (Lu *et al.* 2012; Yang *et al.* 2014).

Crystalline Phase Analyses

The XRD patterns of the pre- and post-sorption biochars are shown in Fig. 2b. Carbon in the biochars existed mainly in amorphous form while quartz and calcite were found in the pre- and post-sorption biochars (Fig. 2b). Quartz and calcite were reported in biochars produced at relatively high temperatures from various feedstocks (Cao *et al.* 2009; Xu *et al.* 2013). Some new peaks occurred in the biochars after Pb sorption (Fig. 2b). The d values and the corresponding 2θ degree of the new peaks were assigned to cerussite ($PbCO_3$). The possible peak of $Pb_3(PO_3)_2$ was noted in the post-sorption MAW, supporting the previous reports of Pb adsorption onto dairy manure biochars (Cao *et al.* 2009; Xu *et al.* 2013). Surface precipitation of $PbCO_3$ phase was also reported when Pb(II) was exposed to calcite in DI water (Rouff *et al.* 2005). Separating Pb(II) removal by biochars into organic and inorganic fractions indicated that the sorption capacities were only around 0.4% to 0.6% for organic fractions and more than 99% for the inorganic fractions (Xu *et al.* 2014). Therefore, surface precipitation may be a significant mechanism responsible for adsorption of Pb onto biochars.

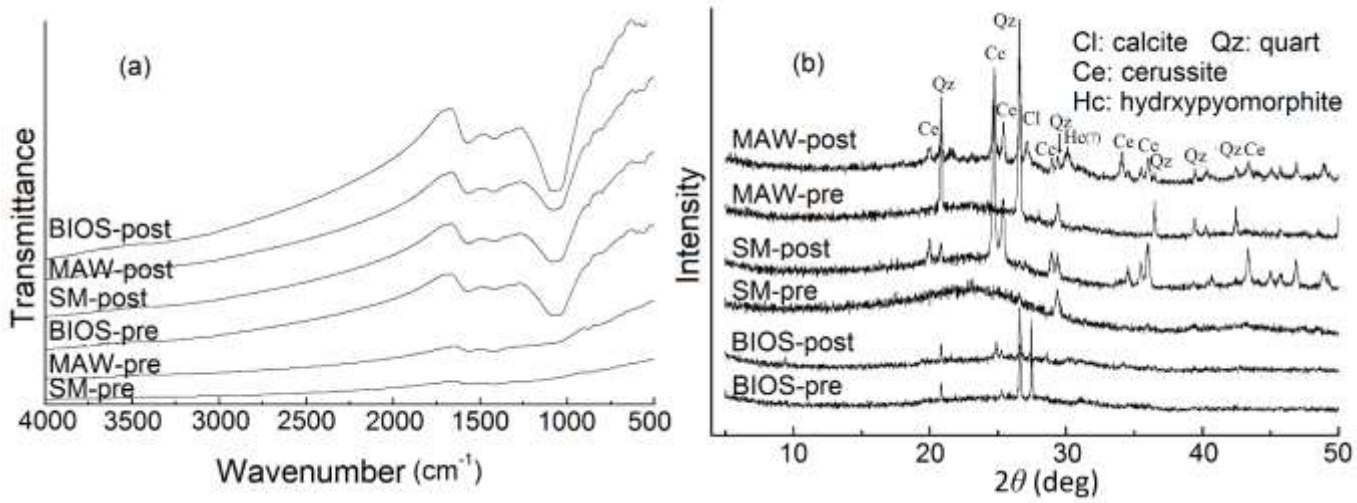

Fig. 2. FT-IR spectra (a) and XRD patterns (b) of the pre- and post-sorption biochars (pre-sorption biochar data are from Wu *et al.* (2016))

Surface Speciation of C, O, and Pb for Adsorption Mechanism Insight

The survey scans of XPS analysis for the pre- and post Pb-sorption biochars (Fig. 3) showed that carbon and oxygen were the dominant elements in the biochar surfaces, while Pb appeared on biochar surfaces after Pb(II) sorption. No mineral elements were found in the pre- and post-sorption biochars in the detection range of XPS (Fig. 3). The presence of Pb_{4d} provides evidence of Pb(II) fixation onto the surface of biochars. The surface Pb contents were in the order of MAW > BIOS > SM (Fig. 3), consistent with the results of batch sorption.

High-resolution XPS spectra of the pre- and post Pb-sorption biochars for C_{1s}, O_{1s} and Pb_{4d} were also analyzed (Fig. 4). Only one dominant peak appeared at the binding energy of around 284.8 eV for C_{1s} and around 533 eV for O_{1s} in the pre- and post Pb-

sorption biochars, which can be ascribed to graphite C for C_{1s} and C–OH or O–C for O_{1s} (Datsyuk *et al.* 2008) (Fig. 4a, b). The lack of significant changes on chemical states of surface carbon and oxygen in biochars observed during the sorption process (Fig. 4a, b) may explain the extremely low sorption capacities of the organic fractions (around 0.4% to 0.6%) for Pb(II) removal as indicated by Xu *et al.* (2014). Two prominent Pb peaks corresponding to $Pb_{4d5/2}$ and $Pb_{4d7/2}$ were found on the surface of biochars after Pb sorption (Fig. 4c). Peaks of $Pb_{4d7/2}$ in BIOS, SM and MAW were found at the binding energy of 138.1eV to 138.4eV (Fig. 4c), which can be associated with $PbCO_3$ (Taylor and Perry 1984). These further confirmed the above-mentioned adsorption mechanism from XRD analyses that surface precipitation was the important mechanism for Pb(II) adsorption onto biochars.

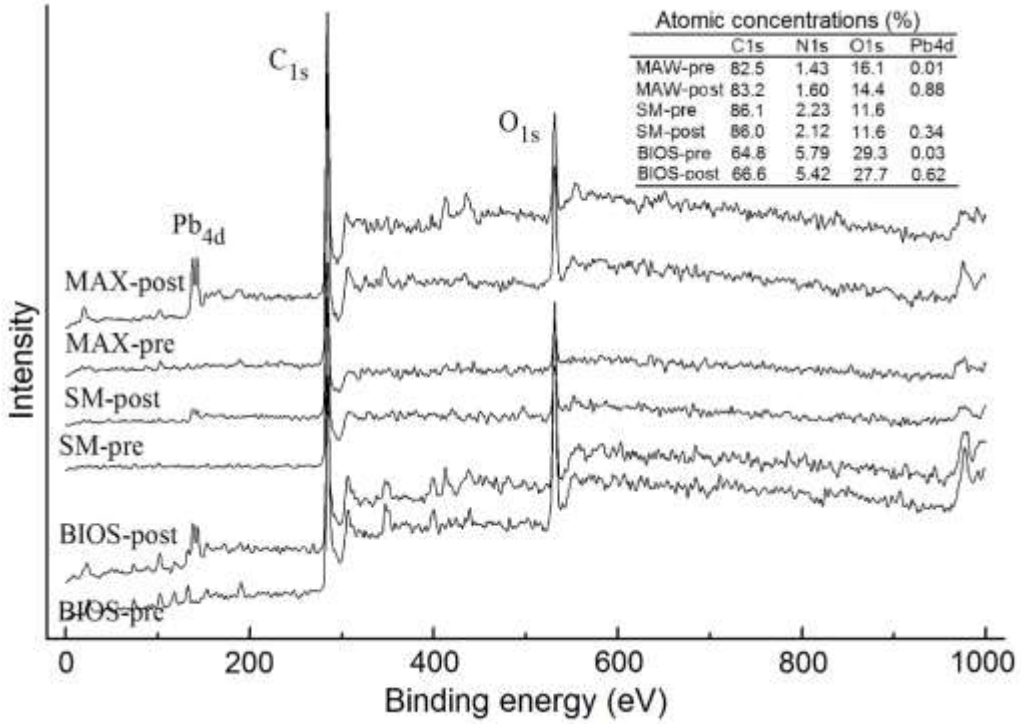

Fig. 3. Survey scan of XPS analysis for the pre- and post-sorption biochars

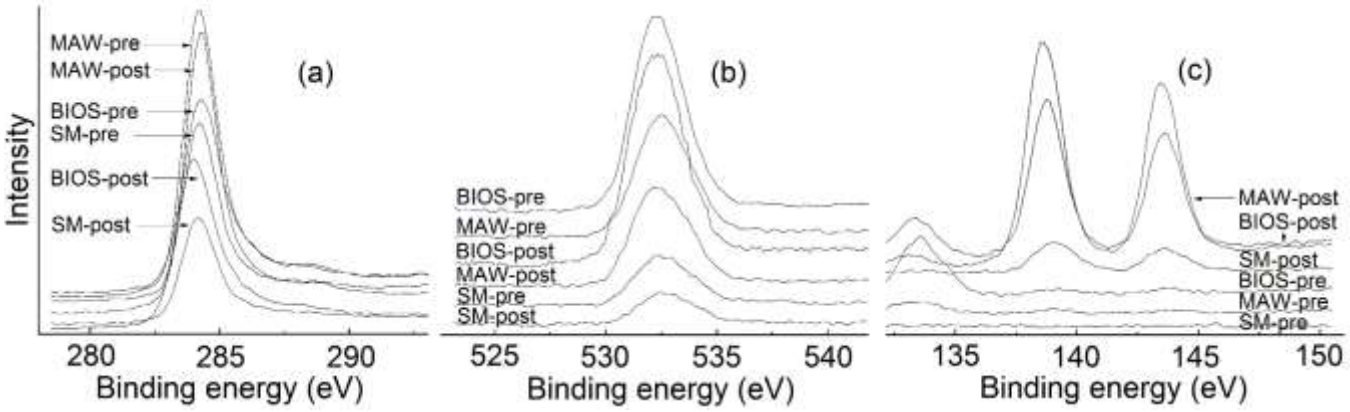

Fig. 4. High-resolution XPS spectra of (a) C_{1s}, (b) O_{1s} and (c) Pb_{4d} in the pre- and post-sorption biochars

CONCLUSIONS

1. Both isotherm and kinetic adsorption showed the highest adsorption capacities of Pb(II) for manure-based biochars, and then sludge- and plant-based biochars. Experimental data of adsorption kinetics and isotherms were well fitted by either the pseudo-first-order or pseudo-second-order kinetic model and by the Langmuir isotherm model, respectively.
2. Multiple characterization of FT-IR, XRD, and XPS for the pre- and post-adsorption biochars revealed the dominant sorption mechanism of the surface precipitation of Pb-carbonate during Pb(II) adsorption onto biochars.

ACKNOWLEDGMENTS

The authors are thankful for the support of the Natural Science Fund of China (21677075).

REFERENCES CITED

Ahmad, M., Rajapaksha, A. U., Lim, J. E., Zhang, M., Bolan, N., Mohan, D., Vithanage, M., Lee, S. S., and Ok, Y. S. (2014). "Biochar as a sorbent for contaminant management in soil and water: A review," *Chemosphere* 99, 19-33. DOI: 10.1016/j.chemosphere.2013.10.071

Cao, X. D., Ma, L. N., Gao, B., and Harris, W. (2009). "Dairy-manure derived biochar effectively sorbs lead and atrazine," *Environ. Sci. Technol.* 43(9), 3285-3291. DOI: 10.1021/Es803092k

Chen, D., Li, R.Y., Bian, R. J., Li, L. Q., Joseph, S., Crowley, D., and Pan, G. X. (2017). "Contribution of soluble minerals in biochar to Pb^{2+} adsorption in aqueous solutions," *Bioresources* 12(1), 1662-1679. DOI: 10.15376/biores.12.1.1662-1679

Chen, W. M., Chen, M. Z., and Zhou, X. Y. (2015). "Characterization of biochar obtained by co-pyrolysis of waste newspaper with high-density polyethylene," *Bioresources* 10(4), 8253-8267. DOI: 10.15376/biores.10.4.8253-8267

Datsyuk, V., Kalyva, M., Papagelis, K., Parthenios, J., Tasis, D., Siokou, A., Kallitsis, I., and Galiotis, C. (2008). "Chemical oxidation of multiwalled carbon nanotubes," *Carbon* 46(6), 833-840. DOI: 10.1016/j.carbon.2008.02.012

Ding, Z. H., Hu, X., Wan, Y. S., Wang, S. S., and Gao, B. (2016a). "Removal of lead, copper, cadmium, zinc, and nickel from aqueous solutions by alkali-modified biochar: Batch and column tests," *J. Ind. Eng. Chem.* 33, 239-245. DOI: 10.1016/j.jiec.2015.10.007

Ding, Z. H., Wan, Y. S., Hu, X., Wang, S. S., Zimmerman, A. R., and Gao, B. (2016b). "Sorption of lead and methylene blue onto hickory biochars from different pyrolysis temperatures: Importance of physicochemical properties," *J. Ind. Eng. Chem.* 37, 261-267. DOI: 10.1016/j.jiec.2016.03.035

Fu, B. M., Ge, C. J., Yue, L., Luo, J. W., Feng, D., Deng, H., and Yu, H. M. (2016). "Characterization of biochar derived from pineapple peel waste and its application for sorption of oxytetracycline from aqueous solution," *BioR esources* 11(4), 9017-

9035. DOI: 10.15376/biores.11.4.9017-9035
Helfferich, F. (1962). *Ion Exchange*, McGraw Hill, New York, USA.
Hu, X., Ding, Z. H., Zimmerman, A. R., Wang, S. S., and Gao, B. (2015). "Batch and column sorption of arsenic onto iron-impregnated biochar synthesized through hydrolysis," *Water Res.* 68, 206-216. DOI: 10.1016/j.watres.2014.10.009
Inyang, M. I., Gao, B., Yao, Y., Xue, Y. W., Zimmerman, A., Mosa, A., Pullammanappallil, P., Ok, Y. S., and Cao, X. D. (2016). "A review of biochar as a low-cost adsorbent for aqueous heavy metal removal," *Crit. Rev. Env. Sci. Tec.* 46(4), 406-433. DOI: 10.1080/10643389.2015.1096880
Liu, Z. G., and Zhang, F. S. (2009). "Removal of lead from water using biochars prepared from hydrothermal liquefaction of biomass," *J. Hazard. Mater.* 167(1-3), 933-939. DOI: 10.1016/j.jhazmat.2009.01.085
Lu, H. L., Zhang, W. H., Yang, Y. X., Huang, X. F., Wang, S. Z., and Qiu, R. L. (2012). "Relative distribution of Pb^{2+} sorption mechanisms by sludge-derived biochar," *Water Res.* 46(3), 854-862. 10.1016/j.watres.2011.11.058
Mohan, D., Pittman, C. U., Bricka, M., Smith, F., Yancey, B., Mohammad, J., Steele, P. H., Alexandre-Franco, M. F., Gomez-Serrano, V., and Gong, H. (2007). "Sorption of arsenic, cadmium, and lead by chars produced from fast pyrolysis of wood and bark during bio-oil production," *J. Colloid. Interf. Sci.* 310(1), 57-73. DOI 10.1016/j.jcis.2007.01.020
Mohan, D., Sarswat, A., Ok, Y. S., and Pittman, C. U. (2014). "Organic and inorganic contaminants removal from water with biochar, a renewable, low cost and sustainable adsorbent - A critical review," *Bioresource Technol.* 160, 191-202. DOI: 10.1016/j.biortech.2014.01.120
Rouff, A. A., Reeder, R. J., and Fisher, N. S. (2005). "Electrolyte and pH effects on Pb(II)-calcite sorption processes: The role of the $PbCO^0_{3(aq)}$ complex," *J. Colloid. Interf. Sci.* 286(1), 61-67. DOI: 10.1016/j.jcis.2005.01.053
Tan, X. F., Liu, Y. G., Zeng, G. M., Wang, X., Hu, X. J., Gu, Y. L., and Yang, Z. Z. (2015). "Application of biochar for the removal of pollutants from aqueous solutions," *Chemosphere* 125, 70-85. DOI: 10.1016/j.chemosphere.2014.12.058
Taylor, J. A., and Perry, D. L. (1984). "An X-ray photoelectron and electron-energy loss study of the oxidation of lead," *J. Vac. Sci. Technol.* A2(2), 771-774. DOI: 10.1116/1.572569
Wu, H., Che, X., Ding, Z., Hu, X., Creamer, A. E., Chen, H., and Gao, B. (2016). "Release of soluble elements from biochars derived from various biomass feedstocks," *Environ. Sci. Pollut. R.* 23(2), 1905-1915. DOI: 10.1007/s11356-015-5451-1
Xu, X. B., Hu, X., Ding, Z. H., Chen, Y. J., and Gao, B. (2017). "Waste-art-paper biochar as an effective sorbent for recovery of aqueous Pb(II) into value-added PbO nanoparticles," *Chem. Eng. J.* 308, 863-871. DOI: 10.1016/j.cej.2016.09.122
Xu, X.Y., Cao, X. D., Zhao, L., Wang, H. L., Yu, H. R., and Gao, B. (2013). "Removal of Cu, Zn, and Cd from aqueous solutions by the dairy manure-derived biochar," *Environ. Sci. Pollut. R* 20(1), 358-368. DOI: 10.1007/s11356-012-0873-5

Xu, X. Y., Cao, X. D., Zhao, L., Zhou, H. J., and Luo, Q. S. (2014). "Interaction of organic and inorganic fractions of biochar with Pb(II) ion: Further elucidation of mechanisms for Pb(II) removal by biochar," *Rsc Adv.* 4(85), 44930-44937. DOI: 10.1039/c4ra07303g

Yang, Y., Wei, Z. B., Zhang, X. L., Chen, X., Yue, D. M., Yin, Q., Xiao, L., and Yang, L. Y. (2014). "Biochar from *Alternanthera philoxeroides* could remove Pb(II) efficiently," *Bioresource Technol.* 171, 227-232. DOI: 10.1016/j.biortech.2014.08.015

Article submitted: April 5, 2017; Peer review completed: July 7, 2017; Revised version received and accepted: July 21, 2017; Published: July 31, 2017.
DOI: 10.15376/biores.12.3.6763-6772